

# Structural MRI-findings in Mild Cognitive Impairment and Alzheimer's Disease

Strukturalne zmiany w MRI u chorych  
z Zespołem Lekkich Zaburzeń Poznawczych  
oraz z chorobą Alzheimerera

Philipp A. Thomann<sup>1</sup>, Johannes Pantel<sup>2</sup>, Torsten Wüstenberg<sup>3</sup>,  
Frederik L. Giesel<sup>4</sup>, Ulrich Seidl<sup>1</sup>, Peter Schönknecht<sup>1</sup>  
Marco Essig<sup>4</sup>, Johannes Schröder<sup>1</sup>

<sup>1</sup> Section of Geriatric Psychiatry, University of Heidelberg, Germany

<sup>2</sup> Department of Psychiatry, J.W. Goethe University, Frankfurt/Main, Germany

<sup>3</sup> Department of Medical Psychology, Georg-August University Goettingen, Germany

<sup>4</sup> German Cancer Research Center, Heidelberg, Germany

**Key words:** mild cognitive impairment, Alzheimer's disease, MRI, structural changes, ROI-measurement, voxel-based morphom

**Słowa kluczowe:** zespół lekkich zaburzeń poznawczych, choroba Alzheimerera MRI, zmiany strukturalne, obszar zainteresowania, morfometria bazująca na metodzie wokseli

## Summary

**Objective.** This study investigates morphological brain changes in subjects with mild cognitive impairment (MCI) and Alzheimer's disease (AD).

**Methods.** 21 subjects with MCI, 21 healthy controls and 10 patients with AD were examined with magnetic resonance imaging (MRI). For the analysis of the MRI data two different methods – region of interest (ROI) – guided manual tracing of predefined neuroanatomical substructures as well as rater-independent voxel-based morphometry (VBM) – were applied.

**Results.** Manual tracing demonstrated a significantly reduced volume of the right parahippocampal gyrus in MCI subjects compared with controls. VBM did not reveal any significant structural differences between those two groups. In AD, both methods revealed significant atrophy of medial temporal lobe substructures (hippocampus, parahippocampal gyrus), the temporal lobe in general and parts of the frontal lobe.

**Conclusion.** Structural brain alterations are already verifiable in the assumed preclinical stage of AD. In the detection of these discrete atrophic changes ROI-based measurement seems to be more sensitive than VBM.

---

### Adres do korespondencji:

Prof. Dr. med. Johannes Schröder  
Section of Geriatric Psychiatry University of Heidelberg  
Voßstr. 4, 69115 Heidelberg, Germany  
Phone: +49-6221-56-5468, Fax: +49-6221-56-5327  
e-mail: johannes\_schroeder@med.uni-heidelberg.de

## Introduction

Alzheimer's disease (AD), the most frequent dementia beyond the age of 65 years, affects an eminent and increasing part of the population. With the availability of modern drug treatment, e.g. cholinesterase-inhibitors, and promising therapeutic options in future (e.g. anti-amyloid strategies), the development of sensitive and specific markers of early AD gains in importance. In a clinical routine setting, structural neuroimaging is mainly used for excluding other pathologies that may cause dementia such as normotensive hydrocephalus, tumor, vascular lesions or infectious diseases [1, 2]. Besides its contribution in distinguishing AD from other causes of dementia, structural neuroimaging - particularly magnetic resonance imaging (MRI) - may be of important value in identifying, among individuals complaining or presenting slight cognitive deficits, those who will progress to manifest AD.

It is generally accepted that most of the subjects who develop AD pass through a stage with minor cognitive deficits which exceed those of the normal physiological aging processes, but are not severe enough to allow a clinical diagnosis of dementia. This transitional phase between health and the onset of AD is commonly referred as mild cognitive impairment (MCI). Previous longitudinal studies demonstrated that MCI subjects have an increased risk to develop the complete clinical picture of AD at observed follow-up [3-5].

Neuropathological research has shown that brain degeneration occurs very early in the course of the disease, even before the onset of clinical symptoms, and predominantly affects certain areas, particularly the substructures of the medial temporal lobe [6-9]. MRI enables the visualization of these early brain changes in vivo. Thus, several neuroimaging studies reported significant atrophy of the hippocampus [10-13], the parahippocampal gyrus [14] and the entorhinal cortex [12, 13, 15-18] in subjects with MCI. In the mentioned studies image analysis was performed using the region of interest (ROI) approach which is based upon the a priori definition of specific brain regions by neuroanatomically skilled raters. ROI analysis constitutes, up to now, the gold standard in brain atrophy measurements, but there are some major disadvantages such as observer/operator dependency, expenditure of time and bias in brain structure and anatomical region boundary selection [19]. So far, the variability of these measurements has limited direct comparison of the results of different research groups. In order to overcome these limitations observer independent computer based tools have been developed that allow automated detection of volume or shape changes throughout the whole brain. Statistical parametric mapping (SPM) software [20] permits the comparison of gray matter density on a voxel by voxel basis in a group of patients with the corresponding variables in a group of controls. The result of such a voxel-based morphometry (VBM) is a three dimensional map displaying significant regional differences in gray matter density, serving as an indirect marker for gray matter atrophy.

Recent VBM studies in AD support the findings of the ROI investigations cited above in that they revealed a significant decrease of gray matter density in the medial temporal lobe [21-24]. Additionally, the cingulate gyrus and the temporoparietal association cortex have been reported to underly atrophic processes [21, 23, 24]. VBM findings in MCI are inconsistent, in so far different studies describe different regions to be predominantly affected [25-27].

As pointed out above, manual segmentation represents an established method in the detection of atrophic processes, while VBM is a promising but still experimental tool. Comparison of the two different techniques is expedient and has still not been performed for MCI and AD. In the present study we therefore investigated MRI scans of subjects with MCI, patients with early AD and healthy controls using both manual tracing and VBM.

## Methods

### Subject selection

Subjects with MCI and cognitively intact control subjects were recruited among the Heidelberg subsample of the interdisciplinary longitudinal study on adult development (ILSE) which is conducted in Heidelberg and Leipzig (Germany). Subjects were selected from the community resident register which is a compulsory register of all residents in Germany. All subjects were screened for health by history, physical

examination, electrocardiogram, and laboratory testing. Cognitive performance was assessed using a previously described extensive neuropsychological test battery [27, 28]. The Heidelberg subsample of ILSE consisted of 252 individuals (birth cohort: 1930-32). Among these individuals, subjects with MCI were identified according to the following criteria of aging-associated cognitive decline (AACD) [29]:

1. Performance of at least 1 standard deviation below the age-adjusted norm on a standardized test of cognition, involving at least one of the following domains: learning and memory, language, attention and cognitive speed, visuoconstructional abilities.
2. Exclusion of any medical, neurological or psychiatric disorder that could produce cognitive deterioration as determined by history and/or clinical examination.
3. Normal activities of daily living
4. Exclusion of dementia

A detailed description of the ILSE study protocol as well as of the applied neuropsychological test battery has been published previously [27, 28].

In order to take account of the temporal stability of the neuropsychological findings, all subjects fulfilling the above-mentioned AACD criteria at baseline ( $n=47$ ) as well as a corresponding number of cognitively unimpaired control subjects (matched for age, gender and educational level) were reinvestigated 30 to 50 month after the first visit and asked for their informed consent to perform an MRI investigation. Thus, 71 subjects of the original ILSE-sample could be reinvestigated clinically, neuropsychologically, and by MRI at follow-up. Cases with significant indications of cerebrovascular disease revealed by MRI, emergence of a neurological/medical condition sufficient to cause cognitive decline, or incomplete/inappropriate MRI-data sets (e.g. withdrawal due to claustrophobia, motion artifacts) were excluded from further analysis. Of the remaining 42 subjects, those who scored below 1 standard deviation in at least one cognitive domain at both visits and/or demonstrated a significant deterioration of test performance during follow-up (without however fulfilling criteria for dementia yet) were included in the AACD/MCI group ( $n=21$ ). Subjects who did not fulfill these requirements were assigned to the cognitively intact control group ( $n=21$ ).

As an additional reference group 10 AD-patients were drawn from a sample of patients consecutively admitted and investigated at the Section of Geriatric Psychiatry (University of Heidelberg). These patients were diagnosed as suffering from AD according to the NINCDS-ADRDA criteria [30] and were matched to the two other groups by age and gender. In order to compare the degree of cognitive impairment between the three study groups the global deterioration scale (GDS) [31] was performed on each subject.

The study was approved by the ethics committee of the Medical Faculty in Heidelberg. Written informed consent was obtained from all participating subjects after the procedures of the study had been fully explained.

### **MRI data acquisition**

The MRI-data were obtained at the German Cancer Research Center with a 1.5-T Magnetom Symphony MR scanner (Siemens Medical Solutions, Erlangen, Germany). To exclude secondary causes of dementia and ischemic changes a 2D T2-weighted Fast-Spin Echo ( $TR = 4500$  ms,  $TE = 90$  ms) sequence was performed in axial orientation. For volumetric analysis a T1-weighted 3D magnetization prepared rapid gradient echo sequence (MP-RAGE) was performed with the following parameters: 126 coronar slices, image matrix =  $256 \times 256$ , voxel size =  $0.98\text{mm} \times 0.98\text{mm} \times 1.8$  mm,  $TR=10$  msec,  $TE=4$  msec.

### **ROI-measurements**

Volumetric measurements included the total intracranial volume (TIV), the whole brain volume (WBV), the CSF volume, as well as volumes of the frontal and temporal lobes, the hippocampal formation, and the parahippocampal gyrus bilaterally. TIV, WBV, CSF-volume and frontal volumes were assessed semi-automatically using the software NMRWin as has been described previously [32-34].

The volumes of the temporal lobes were manually traced bilaterally on 45-50 consecutive coronal T1-weighted sections. A detailed description of the standardized measurement protocol and tracing guidelines has been published previously [32,35]

Volumes of the hippocampal formation and the parahippocampal gyrus were manually traced bilaterally for each subject on 30-35 consecutive T1-weighted sections. The term hippocampal formation refers to a constellation of anatomically distinct structures, including the subiculum, Ammon's horn (hippocampus proper), and the dentate gyrus. Because these structures were nearly indistinguishable visually on the MR images, they were sampled as a whole complex. Hippocampal measures were initiated 3 slices rostrally to the point of fusion of the pedunculi cerebri and the pons. Caudally, outlining of the hippocampal formation was terminated at the level where the fornix and the hippocampus fuse. Thus, small proportions of the anterior (head) and posterior (tail) parts of the hippocampal formation were not sampled. Using the above described rostral and caudal boundaries however, facilitated a standardised sampling of the hippocampal formation on those slices, bearing the hippocampus clearly demarcated from adjacent brain structures. This avoided ambiguities with respect to the separation of the structure from the amygdala (head) and the pulvinar thalami (tail) and improved the reliability of the measurement.

Volume measures of the parahippocampal gyrus were sampled on the same slices as the hippocampal measures. Thus, in analogy to the hippocampal measurement, small samples of its most rostral part (where it is fused with the uncus) and its most caudal part (where the transition to the lingual gyrus takes place) were not considered. Outlining of the parahippocampal gyrus started laterally in the depth of the collateral sulcus. The parahippocampal gyrus was followed along its inferior and medial boarder (where it is clearly demarcated from the adjacent CSF of the ambient or peri-mesencephalic cistern) up to the uncus sulcus. From there the inferior boarder of the subiculum (which itself is included in the hippocampal measures) served as the superior demarcation line until the most medial part of the temporal stem was reached. Finally, a straight line was drawn to the starting point in the collateral sulcus separating the parahippocampal gyrus from the adjacent temporal lobe.

Intrarater reliability for the total intracranial and whole brain volume determination was significant, according to the intercorrelation coefficient ( $r_{tt} = 0.98$ ;  $p < 0.0005$ ). In order to demonstrate the reproducibility of the manual tracing method, all measurement were performed twice by the same rater blinded for group membership. This yielded intercorrelation coefficients of  $r_{tt} = 0.98$  (frontal lobes), and  $r_{tt} = 0.99$  (temporal lobes bilaterally),  $p < 0.0005$ . In addition, interrater reliabilities for determination of volumes for the medial temporal lobe regions of interest were determined in a subset of 16 randomly selected subjects, considering one set of traces as the "gold standard". The traces that were considered to be the "gold standard" were generated by one of the authors with a solid experience and expertise in medial temporal lobe measurements (J.P.). This approach yielded intercorrelation coefficients of  $r_{tt} = 0.98$  (right hippocampus),  $r_{tt} = 0.97$  (left hippocampus and right parahippocampal gyrus), and  $r_{tt} = 0.96$  (left parahippocampal gyrus), respectively ( $p < 0.0005$  for all the regions of interest).

### **Statistical analysis of ROI-measurements**

All computations were performed using the statistical analysis system (SAS / SAS-Institute, version 9.1.2). To address potential interindividual differences in head size, all volumetric data were corrected by dividing each raw value by the subject's TIV. Analyses of variance with Duncan's tests were calculated in order to compare the volumetric data between the diagnostic groups. The gender distribution was analyzed by the  $\chi^2$ -test.

### **VBM-analysis**

In VBM-analysis, the anatomical datasets were segmented into gray matter (GM), white matter (WM) and cerebro spinal fluid (CSF), applying the iterative a-priori knowledge based algorithm implemented in SPM99 software (<http://www.fil.ion.ucl.ac.uk/spm>).

VBM was used to perform statistical inferences about differences in tissue distribution in space. Therefore brain segments were normalised (1mm x 1mm x 1mm) into standard stereotaxic space (T1-

-template provided by the Montreal Neurological Institute) and smoothed using a 10mm full-width at half-maximum Gaussian kernel. Two sample t-tests were calculated for each group comparison. Only results surviving a threshold of  $p < 0.05$  (corrected for multiple comparisons) and a cluster size equal or greater than 1000 voxel will be reported.

## Results

### Results of manual tracing

A comparison of the clinical characteristic and volumetric measures of the three investigated groups is displayed in table 1. According to the statistical analysis there were no significant differences with respect to age, gender distribution, and level of school education. In addition, the TIV did not differ significantly between the groups ( $F = 0.49$ ;  $df = 2,49$ ;  $p = 0.67$ ). Comparison of the remaining volumetric parameters was based on the corrected values. Subjects with AACD/MCI showed a significantly lower volume of the right parahippocampal gyrus (-12%;  $F = 18.02$ ;  $df = 2,49$ ;  $p < 0.0005$ ) when compared to the cognitively intact control group. On the left side, mean parahippocampal gyrus of the AACD/MCI group was 7% smaller when compared to controls, although this difference did not reach statistical significance. By contrast, AD-patients showed a significant bilateral volume reduction of the parahippocampal gyrus (right:  $F = 18.02$ ;  $df = 2,49$ ;  $p < 0.0001$ ; left:  $F = 14.4$ ;  $df = 2,49$ ;  $p < 0.0001$ ) when compared to both the AACD group (right: -18%; left: -22.8%) and the cognitively intact control group (right: -28%; left: -29.6%).

The WBV, the CSF volumes as well as the frontal, temporal, and hippocampal volumes of the AACD/MCI subjects were not significantly different when compared to the cognitively intact subjects. In contrast, the AD patients were characterized by significantly smaller frontal as well as hippocampal and temporal lobe volumes bilaterally in comparison to both the AACD and control group (frontal:  $F = 4.1$ ;  $df = 2,49$ ;  $p < 0.05$ ; temporal right:  $F = 8.6$ ;  $df = 2,49$ ;  $p < 0.005$ ; temporal left:  $F = 8.5$ ;  $df = 2,49$ ;  $p < 0.005$ ; hippocampus right:  $F = 13.5$ ,  $df = 2,49$ ;  $p < 0.0005$ ; hippocampus left:  $F = 28.4$ ;  $df = 2,49$ ;  $p < 0.0005$ ).

### Results of VBM-analysis

In Table 2 the results of the comparison between AD patients and healthy controls are summarized. Most significant decrease in gray matter density was found in the anterior part of the cingulate gyrus bilaterally, the right superior temporal sulcus, the left inferior frontal sulcus and the hippocampus bilaterally. Figure 1 illustrates the results of the VBM analysis. No significant difference in gray matter density was found in AACD/MCI subjects when compared to healthy controls.

## Discussion

The present MRI study demonstrates – with regard to manual tracing – a significant volume reduction in the parahippocampal gyrus in elderly subjects suffering from MCI. Consistent though much more pronounced changes were found in AD patients, indicating that with respect to parahippocampal gyrus volumes MCI subjects take an intermediate position between AD patients and cognitively intact controls.

These findings are in line with neuropathological studies demonstrating that three main stages can be differentiated during the clinical course of AD (4, 5, 6): In the earliest and almost symptom-free transentorhinal stage, morphological changes selectively affect the parahippocampal regions. The destructive process then spreads into additional structures of the medial temporal lobe/limbic system, especially involving the hippocampal formation (limbic stage). Eventually, the pathological alterations encroach the isocortex until major parts of the temporal, parietal, and frontal cortical areas are affected (isocortical stage). Clinically, the isocortical stage is associated with a moderate to severe dementia syndrome. In view of this neuropathological evidence, it is conceivable that the parahippocampal volume reduction that we observed in the mildly cognitively impaired group reflects degenerative atrophic changes that may correspond to the earliest morphological alterations as they were described for the preclinical (transentorhinal) stages of AD [6-8].

**Table 1.** Clinical characteristic and (corrected) volumetric variables in mild cognitive impairment/AACD, Alzheimer's disease, and cognitively intact control subjects. Results of an analysis of variance (Duncan's test on the 5% level)

**Tab. 1.** Zestawienie cech klinicznych i wartości zmiennych objętościowych u osób z zespołem lekkich zaburzeń poznawczych (MCI) i chorobą Alzheimera (AD) oraz w grupie kontrolnej bez zaburzeń poznawczych. Wyniki analizy wariancji (test Duncana na poziomie 5%)

|                                | 1<br>controls            | 2<br>MCI                 | 3<br>AD                  | F    | Duncan's<br>Test (5%) |
|--------------------------------|--------------------------|--------------------------|--------------------------|------|-----------------------|
| <b>N</b>                       | 21                       | 21                       | 10                       |      |                       |
| <b>Age<br/>(years)</b>         | 66.19 ( $\pm 0.75$ )     | 66.57 ( $\pm 0.60$ )     | 66.00 ( $\pm 7.66$ )     | 0.87 | n.sig.                |
| <b>Sex<br/>(m/f)</b>           | 10/11                    | 11/10                    | 6 / 4                    |      | n.sig. 1              |
| <b>Education<br/>(years)</b>   | 10.1 ( $\pm 1.7$ )       | 9.5 ( $\pm 1$ )          | 10.0 ( $\pm 1.5$ )       | 0.9  | n.sig.                |
| <b>GDS</b>                     | 1,29 ( $\pm 0.46$ )      | 1,71 ( $\pm 0.46$ )      | 3.90 ( $\pm 0.88$ )      | 95.9 | 1 < 2 < 3             |
| <b>MMSE</b>                    | n.d.                     | n.d.                     | 19.2 ( $\pm 3.85$ )      | n.d. | n.d.                  |
| <b>TIV (cm<sup>3</sup>)</b>    | 1268 ( $\pm 144$ )       | 1230.9 ( $\pm 110$ )     | 1260 ( $\pm 170$ )       | 0.41 | n.sig.                |
| <b>WB</b>                      | 0.7 ( $\pm 0.04$ )       | 0.69 ( $\pm 0.025$ )     | 0.67 ( $\pm 0.040$ )     | 2.8  | 1 > 3                 |
| <b>CSF</b>                     | 0.3 ( $\pm 0.04$ )       | 0.31 ( $\pm 0.025$ )     | 0.33 ( $\pm 0.040$ )     | 2.1  | n.sig.                |
| <b>Frontal lobes</b>           | 0.065 ( $\pm 0.0097$ )   | 0.066 ( $\pm 0.0095$ )   | 0.056 ( $\pm 0.0072$ )   | 4.2  | 1, 2 > 3              |
| <b>Temporal<br/>lobe Right</b> | 0.038 ( $\pm 0.004$ )    | 0.037 ( $\pm 0.0029$ )   | 0.032 ( $\pm 0.0044$ )   | 8,6  | 1, 2 > 3              |
| <b>Temporal<br/>lobe Left</b>  | 0.036 ( $\pm 0.0033$ )   | 0.035 ( $\pm 0.0047$ )   | 0.030 ( $\pm 0.0021$ )   | 8,5  | 1, 2 > 3              |
| <b>Hippocampus<br/>right</b>   | 0.0024 ( $\pm 0.00039$ ) | 0.0023 ( $\pm 0.00048$ ) | 0.0016 ( $\pm 0.00033$ ) | 13.5 | 1, 2 > 3              |
| <b>Hippocampus<br/>left</b>    | 0.0023 ( $\pm 0.00029$ ) | 0.0024 ( $\pm 0.00043$ ) | 0.0014 ( $\pm 0.00025$ ) | 28.4 | 1, 2 > 3              |
| <b>PHG right</b>               | 0.0025 ( $\pm 0.0003$ )  | 0.0022 ( $\pm 0.0003$ )  | 0.0019 ( $\pm 0.00033$ ) | 18.0 | 1 > 2 > 3             |
| <b>PHG left</b>                | 0.0027 ( $\pm 0.00044$ ) | 0.0025 ( $\pm 0.00041$ ) | 0.0018 ( $\pm 0.00033$ ) | 14.4 | 1, 2 > 3              |

AACD: aging-associated cognitive decline; AD: Alzheimer's disease; GDS: Global Deterioration Scale; MMSE: Mini Mental State Examination; TIV: total intracranial volume; WB: whole brain; CSF: cerebrospinal fluid; PHG: parahippocampal gyrus; n.d.: not done; n.sig.: not significant; 1  $\chi$ -test

**Table 2.** Anatomical structures with significant loss of gray matter density in AD-patients compared to healthy control subjects ( height threshold  $p < 0.05$  (corr.), extent threshold  $k = 1000 \text{ mm}^3 = 1000 \text{ voxels}$ ).**Tab. 2.** Wykaz struktur anatomicznych, w których stwierdzono znacznie zmniejszoną gęstość istoty szarej u chorych z AD w porównaniu do grupy kontrolnej osób zdrowych (próg wysokości  $p < 0.05$  (skoryg.), próg zasięgu  $k = 1000$ 

|    | Anatomical structure                     | Hem.  | Cluster<br>[mm <sup>3</sup> ] | T    | MNI-coordinates<br>x,y,z [mm] |     |     |
|----|--|-------|-------------------------------|------|-------------------------------|-----|-----|
| 1  | Cingulate gyrus (anterior part)          | L/R   | 14629                         | 7.37 | -1                            | 37  | 33  |
|    | Medial frontal gyrus (anterior part)     |       |                               | 4.98 | -2                            | 53  | 17  |
| 2  | Superior temporal sulcus                 | R     | 9241                          | 7.19 | 52                            | -34 | 2   |
|    | Superior temporal gyrus                  |       |                               | 5.74 | 64                            | -40 | 9   |
| 3  | Inferior frontal sulcus                  | L     | 3644                          | 6.70 | -46                           | 15  | 35  |
|    | Superior temporal gyrus                  |       |                               | 4.11 | -53                           | 17  | 8   |
|    | Inferior frontal gyrus (triangular part) |       |                               | 3.88 | -53                           | 13  | 19  |
| 4  | Hippocampus                              | L     | 4946                          | 6.06 | -31                           | -19 | -13 |
|    | Amygdala                                 |       |                               | 5.20 | -26                           | 0   | -20 |
| 5  | Hippocampus                              | R     | 2724                          | 5.72 | 29                            | -10 | -14 |
| 6  | Middle frontal gyrus                     | R     | 2997                          | 5.37 | 46                            | 16  | 42  |
|    | Inferior frontal gyrus (triangular part) |       |                               | 4.11 | 56                            | 14  | 28  |
| 7  | Ventral striatum / Caudate nucleus       | L / R | 3226                          | 5.06 | -3                            | 7   | 7   |
| 8  | Cingulate sulcus / Precuneus             | L / R | 1086                          | 4.91 | 4                             | -49 | 38  |
| 9  | Middle temporal gyrus                    | L     | 4508                          | 4.59 | -59                           | -10 | -11 |
|    | Superior temporal gyrus                  |       |                               | 4.12 | -65                           | -32 | 10  |
| 10 | Inferior frontal gyrus                   | R     | 7218                          | 4.44 | 48                            | 21  | 3   |
| 11 | Postcentral gyrus (inferior part)        |       |                               | 4.37 | 45                            | -10 | 16  |
| 12 | Occipito-parietal sulcus                 | L     | 9205                          | 4.38 | -44                           | -56 | 13  |
|    | Inferior parietal lobule                 |       |                               | 4.36 | -61                           | -35 | 29  |
| 13 | Inferior frontal gyrus                   | L     | 1651                          | 4.14 | -39                           | 19  | -6  |
| 14 | Postcentral gyrus                        | R     | 1145                          | 4.09 | 64                            | -20 | 32  |
|    | Inferior parietal lobule                 |       |                               | 3.60 | 62                            | -28 | 33  |
|    | Thalamus                                 | L     | 2948                          | 3.70 | -10                           | -22 | 11  |
| 15 | Precentral gyrus                         | R     | 2301                          | 3.59 | 48                            | -10 | 45  |
| 16 | Inferior parietal lobule                 | R     | 1398                          | 3.51 | 52                            | -53 | 48  |
| 17 | Intraparietal sulcus                     |       |                               | 3.22 | 36                            | -50 | 51  |

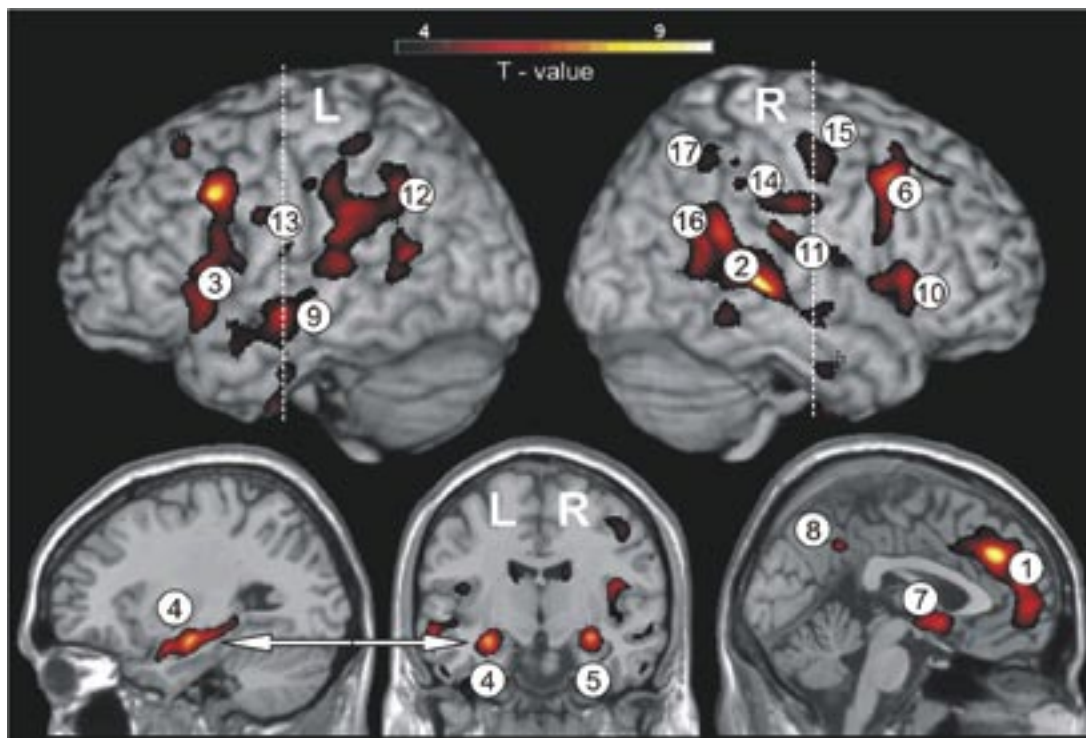


**Fig. 1.** Brain regions showing significant loss of gray matter density in AD patients compared to healthy controls superimposed onto a T1-weighted standard anatomic template (height threshold  $p < 0.05$  (corr.), extent threshold  $k = 1000 \text{ mm}^3 = 1000 \text{ voxels}$ ). Reader's right is subjects' right. Labels correspond to numbering in table 2. The dashed lines indicate the cut direction for the coronar slice in the lower row. The arrows between the coronar and the left sagittal slice point to the left hippocampal region

**Ryc. 1.** Obszary mózgu, w których stwierdzono znacznie zmniejszoną gęstość u chorych z AD w porównaniu do grupy kontrolnej osób zdrowych. Obraz nakładany na standardowym szablonie anatomicznym w widoku T1-zależnym. (próg wysokości  $p < 0.05$  (skoryg.), próg zasięgu  $k = 1000 \text{ mm}^3 = 1000 \text{ wokselów}$ ). Prawa strona obrazu odpowiada prawej stronie osoby badanej. Etykiety nałożono zgodnie z ponumerowaniem w Tabeli 2. Przerwane linie wyznaczają kierunek przekroju dla projekcji koronowej w dolnym rzędzie. Strzałki pomiędzy przekrojami koronalnymi a lewymi sagitalnymi wskazują na okolicę lewego hipokampa

In AD, VBM analysis revealed the substructures of the medial temporal lobe as well as the anterior cingulate gyrus and temporoparietal neocortical areas to undergo atrophic changes. These findings are generally in line with our results from the manual tracing approach. Moreover, they strongly support the results of several other research groups using either ROI-based approaches or VBM [21-24, 36].

In contrast to manual tracing, VBM was not able to detect structural changes in MCI subjects compared to healthy controls. This observation is contradictory to some recently published VBM studies that reported measurable loss of gray matter density in MCI in certain brain regions [25, 26]. This divergent result may be related to aspects of sample selection: Most importantly, our sample consisted of randomly selected subjects drawn from a population based sample, whereas the above mentioned studies analyzed MRI-scans of on demand patients which might have been already in a more advanced stage of their disorder.

Nonetheless, our findings lead to the hypothesis that manual tracing is more sensitive to discrete structural changes, as this technique could, in contrast to VBM, successfully differentiate subjects with MCI from healthy controls. The sensitivity of the VBM algorithm might be diminished by normalization errors, segmentation inaccuracy and smoothing effects. To address these potential methodological limitations, further studies – comparing the different techniques – are needed. Furthermore, we would like to underline that VBM relies on the application of a t-test as the fundamental statistical tool which makes it unsuitable for the comparison of single subjects with a normative template. Accordingly, this



approach solely allows group comparisons. In contrast, ROI-based measures can be used to estimate atrophy in individual cases which makes it more suitable for diagnostic purposes (e.g. within a memory clinic setting). Despite these restrictions, VBM is a time-efficient, almost fully automatic and therefore observer independent method which was useful in revealing morphological differences between patients with mild to moderate AD and healthy controls.

## References

- [1] **Scheltens P.** Early diagnosis of dementia: neuroimaging. *J Neurol*; 1999, 246:16-20.
- [2] **Frisoni GB.** Structural imaging in the clinical diagnosis of Alzheimer's disease: problems and tools. *J Neurol Neurosurg Psychiatry*, 2001, 70:711-8.
- [3] **Jack CR, Jr., Petersen RC, Xu YC, O'Brien PC, Smith GE, Ivnik RJ, Boeve BF, Waring SC, Tangalos EG, Kokmen E.** Prediction of AD with MRI-based hippocampal volume in mild cognitive impairment. *Neurology*; 1999, 52:1397-403.
- [4] **Petersen RC, Smith GE, Waring SC, Ivnik RJ, Tangalos EG, Kokmen E.** Mild cognitive impairment: clinical characterization and outcome. *Arch Neurol*, 1999, 56:303-8.
- [5] **Ritchie K, Artero S, Touchon J.** Classification criteria for mild cognitive impairment: a population-based validation study. *Neurology*, 2001, 56:37-42.
- [6] **Braak H, Braak E.** Neuropathological staging of Alzheimer-related changes. *Acta Neuropathol (Berl)*; 1991, 82:239-59.
- [7] **Mizutani T, Kasahara M.** Hippocampal atrophy secondary to entorhinal cortical degeneration in Alzheimer-type dementia. *Neurosci Lett*; 1997, 222:119-22.
- [8] **Delacourte A, David JP, Sergeant N, Buee L, Wattez A, Vermersch P, Ghzali F, Fallet-Bianco C, Pasquier F, Lebert F, Petit H, Di Menza C.** The biochemical pathway of neurofibrillary degeneration in aging and Alzheimer's disease. *Neurology*, 1999, 52:1158-65.
- [9] **Van Hoesen GW, Augustinack JC, Dierking J, Redman SJ, Thangavel R.** The parahippocampal gyrus in Alzheimer's disease. Clinical and preclinical neuroanatomical correlates. *Ann N Y Acad Sci* 911:254-74.
- [10] **Bottino CM, Castro CC, Gomes RL, Buchpiguel CA, Marchetti RL, Neto MR.** Volumetric MRI measurements can differentiate Alzheimer's disease, mild cognitive impairment, and normal aging. *Int Psychogeriatr*; 2002, 14:59-72.
- [11] Hippocampal formation glucose metabolism and volume losses in MCI and AD. *Neurobiol Aging*, 2001, 22:529-39.
- [12] **Dickerson BC, Goncharova I, Sullivan MP, Forchetti C, Wilson RS, Bennett DA, Beckett LA, deToledo-Morrell L.** MRI-derived entorhinal and hippocampal atrophy in incipient and very mild Alzheimer's disease. *Neurobiol Aging*; 2001, 22:747-54.
- [13] **Du AT, Schuff N, Amend D, Laakso MP, Hsu YY, Jagust WJ, Yaffe K, Kramer JH, Reed B, Norman D, Chui HC, Weiner MW.** Magnetic resonance imaging of the entorhinal cortex and hippocampus in mild cognitive impairment and Alzheimer's disease. *J Neurol Neurosurg Psychiatry*; 2001, 71:441-7.
- [14] **Pantel J, Kratz B, Essig M, Schröder J.** Parahippocampal volume deficits in subjects with aging-associated cognitive decline. *Am J Psychiatry*; 2003, 160:379-82.
- [15] **De Toledo-Morrell L, Goncharova I, Dickerson B, Wilson RS, Bennett DA.** From healthy aging to early Alzheimer's disease: in vivo detection of entorhinal cortex atrophy. *Ann N Y Acad Sci*; 2000, 911:240-53.
- [16] **Juottonen K, Laakso MP, Insausti R, Lehtovirta M, Pitkanen A, Partanen K, Soininen H.** Volumes of the entorhinal and perirhinal cortices in Alzheimer's disease. *Neurobiol Aging*; 1998, 19:15-22.
- [17] **Killiany RJ, Hyman BT, Gomez-Isla T, Moss MB, Kikinis R, Jolesz F, Tanzi R, Jones K, Albert MS.** MRI measures of entorhinal cortex vs hippocampus in preclinical AD. *Neurology*; 2002, 58:1188-96.
- [18] **Xu Y, Jack CR, Jr., O'Brien PC, Kokmen E, Smith GE, Ivnik RJ, Boeve BF, Tangalos RG, Petersen RC.** Usefulness of MRI measures of entorhinal cortex versus hippocampus in AD. *Neurology*; 2000, 54:1760-7.
- [19] **Pruessner JC, Li LM, Serles W, Pruessner M, Collins DL, Kabani N, Lupien S, Evans AC.** Volumetry of hippocampus and amygdala with high-resolution MRI and three-dimensional analysis software: minimizing the discrepancies between laboratories. *Cereb Cortex*; 2000, 10:433-42.

- [20] **Frackowiak RSJ, Friston KJ, Frith CD, Dolan R, Maziotta JC.** Human brain function. Academic Press; 1997.
- [21] **Baron JC, Chetelat G, Desgranges B, Perchev G, Landeau B, de la Sayette V, Eustache F.** In vivo mapping of gray matter loss with voxel-based morphometry in mild Alzheimer's disease. *Neuroimage*; 2001, 14:298-309.
- [22] **Busatto GF, Garrido GE, Almeida OP, Castro CC, Camargo CH, Cid CG, Buchpiguel CA, Furuie S, Bottino CM.** A voxel-based morphometry study of temporal lobe gray matter reductions in Alzheimer's disease. *Neurobiol Aging*; 2003, 24:221-31.
- [23] **Frisoni GB, Testa C, Zorzan A, Sabattoli F, Beltramello A, Soininen H, Laakso MP.** Detection of gray matter loss in mild Alzheimer's disease with voxel based morphometry. *J Neurol Neurosurg Psychiatry*; 2002, 73:657-64.
- [24] **Karas GB, Burton EJ, Rombouts SA, van Schijndel RA, O'Brien JT, Scheltens P, McKeith IG, Williams D, Ballard C, Barkhof F.** A comprehensive study of gray matter loss in patients with Alzheimer's disease using optimized voxel-based morphometry. *Neuroimage*; 2003, 18:895-907.
- [25] **Chetelat G, Desgranges B, De La Sayette V, Viader F, Eustache F, Baron JC.** Mapping gray matter loss with voxel-based morphometry in mild cognitive impairment. *Neuroreport*; 2002, 13:1939-43.
- [26] **Karas GB, Scheltens P, Rombouts SA, Visser PJ, van Schijndel RA, Fox NC, Barkhof F.** Global and local gray matter loss in mild cognitive impairment and Alzheimer's disease. *Neuroimage*; 2004, 23:708-16.
- [27] **Martin P, Martin M.** Design und Methodik der Interdisziplinären Längsschnittstudie des Erwachsenenalters, in: *Aspekte der Entwicklung im mittleren und höheren Lebensalter. Ergebnisse der Interdisziplinären Längsschnittstudie des Erwachsenenalters (ILSE)*. Edited by Martin P, Ettrich KU, Lehr U, Roether D, Martin M, Fischer-Cyrlus A. Darmstadt, Steinkopff:17-27, 2000.
- [28] **Schönknecht P., Pantel J., Kruse A., Schröder J.** Prevalence and natural course of aging-associated cognitive decline in a population based sample of "young-old" subjects. *Am J. Psychiatry*: (in press).
- [29] Aging-associated cognitive decline. Working Party of the International Psychogeriatric Association in collaboration with the World Health Organization. *Int Psychogeriatr*, 1994, 6:63-8.
- [30] **McKhann G, Drachman D, Folstein M, Katzman R, Price D, Stadlan EM.** Clinical diagnosis of Alzheimer's disease: report of the NINCDS-ADRDA Work Group under the auspices of Department of Health and Human Services Task Force on Alzheimer's Disease. *Neurology*, 1984, 34:939-44.
- [31] **Reisberg B, Ferris SH, de Leon MJ, Crook T.** The Global Deterioration Scale for assessment of primary degenerative dementia. *Am J Psychiatry*, 1982, 139:1136-9.
- [32] **Pantel J, Schröder J, Schad LR, Friedlinger M, Knopp MV, Schmitt R, Geissler M, Bluml S, Essig M, Sauer H.** Quantitative magnetic resonance imaging and neuropsychological functions in dementia of the Alzheimer type. *Psychol Med*, 1997, 27:221-9.
- [33] **Friedlinger M, Schad LR, Bluml S, Tritsch B, Lorenz WJ.** Rapid automatic brain volumetry on the basis of multispectral 3D MR imaging data on personal computers. *Comput Med Imaging Graph*, 1995, 19:185-205.
- [34] **Friedlinger M, Schröder J, Schad LR.** Ultra-fast automated brain volumetry based on bispectral MR imaging data. *Comput Med Imaging Graph*, 1999, 23:331-7.
- [35] **Pantel J, Schröder J, Essig M, Jauss M, Schneider G, Eysenbach K, von Kummer R, Baudendistel K, Schad LR, Knopp MV.** In vivo quantification of brain volumes in subcortical vascular dementia and Alzheimer's disease. An MRI-based study. *Dement Geriatr Cogn Disord*, 1998, 9:309-16.
- [36] **Pantel J, Schönknecht P, Essig M, Schröder J.** Distribution of cerebral atrophy assessed by magnetic resonance imaging reflects patterns of neuropsychological deficits in Alzheimer's dementia. *Neurosci Lett*, 2004, 361:17-20.

**Otrzymano / Received** 14.03.2005

**Zrecenzowano / Reviewed** 28.03.2005

**Zatwierdzono do druku / Accepted** 30.03.2005